

Published in final edited form as:

*J Med Chem.* 2010 November 11; 53(21): 7796–7803. doi:10.1021/jm1009555.

## Cationic porphycenes as potential photosensitizers for antimicrobial photodynamic therapy

Xavier Ragàs<sup>†,‡</sup>, David Sánchez-García<sup>†</sup>, Rubén Ruiz-González<sup>†</sup>, Tianhong Dai<sup>‡,⊥</sup>,  
Montserrat Agut<sup>†</sup>, Michael R. Hamblin<sup>‡,⊥,#</sup>, and Santi Nonell<sup>\*,†</sup>

<sup>†</sup>Institut Químic de Sarrià, Universitat Ramon Llull, Barcelona 08017, Spain

<sup>‡</sup>Wellman Center for Photomedicine, Massachusetts General Hospital, Boston, Massachusetts 02114, USA

<sup>⊥</sup>Department of Dermatology, Harvard Medical School, Boston, Massachusetts 02115, USA

<sup>#</sup>Harvard-MIT Division of Health Sciences and Technology, Cambridge, Massachusetts 02139, USA

### Abstract

Structures of typical photosensitizers used in antimicrobial photodynamic therapy are based on porphyrins, phthalocyanines and phenothiazinium salts, with cationic charges at physiological pH values. However derivatives of the porphycene macrocycle (a structural isomer of porphyrin) have barely been investigated as antimicrobial agents. Therefore, we report the synthesis of the first tricationic water-soluble porphycene and its basic photochemical properties. We successfully tested it for *in vitro* photoinactivation of different Gram-positive and Gram-negative bacteria, as well as a fungal species (*Candida*) in a drug-dose and light-dose dependent manner. We also used the cationic porphycene *in vivo* to treat an infection model comprising mouse 3<sup>rd</sup> degree burns infected with a bioluminescent methicillin-resistant *Staphylococcus aureus* strain. There was a 2.6-log<sub>10</sub> reduction ( $p < 0.001$ ) of the bacterial bioluminescence for the PDT-treated group after irradiation with 180 J·cm<sup>-2</sup> of red light.

### Introduction

Antimicrobial photodynamic therapy (APDT)<sup>1</sup> is being actively studied as a possible alternative to antibiotic treatment for localized infections.<sup>2, 3</sup> The basic principles are well understood: in essence, the interaction between light and photoactive drugs, usually called photosensitizers (PSs), forms reactive oxygen species (ROS) created through either electron transfer (type I) or energy transfer (type II) reactions.<sup>4</sup> These ROS will react with many cellular components that will induce oxidative processes leading to cell death.<sup>5-7</sup>

PSs belonging to a variety of chemical structures have been used to inactivate microbial cells, most of them were porphyrin-based,<sup>8</sup> phthalocyanine-based<sup>9</sup> or phenothiazinium-based.<sup>10</sup> Porphycene, a structural porphyrin isomer, is endowed with favorable photophysics that allows it to act as a photodynamic agent,<sup>11</sup> but has rarely been used in the field of APDT. The only two studies using polylysine-porphycene conjugates<sup>12, 13</sup> showed promising results but that research was not pursued, likely due to the lengthy and complex

\*Corresponding author: Phone: +34932672000. Fax: +34932056266. santi.nonell@iqs.url.edu.

**Supporting information available** <sup>1</sup>H-NMR and <sup>13</sup>C-NMR spectra of porphycenes **2** and **3**. HPLC analysis of porphycene **3**. Figures of the calculation of the fluorescence quantum yields and energy-dose experiments for *in vitro* photodynamic inactivation. Methodology for the calculation of singlet oxygen quantum yields.

synthesis of the porphycene macrocycle available at that time, needed to obtain the polymer conjugate. The recent discovery in our laboratory of a straightforward, four-step synthesis of porphycenes<sup>14</sup> provides an opportunity for the assessment of the potential of these compounds in APDT.

The use of outer wall-disrupting agents, such as EDTA<sup>15</sup> or cationic polypeptide polymixin B,<sup>8, 16</sup> and the conjugation of the PS with polymers,<sup>17</sup> nanoparticles,<sup>18</sup> or biomolecules,<sup>19</sup> provides a higher affinity of the PSs against microbial cells. Nevertheless, the discovery that positively charged PSs at physiological pH values promote the photoinactivation of microbial cells<sup>20-22</sup> has stimulated the development of new synthetic routes to develop new useful cationic PSs for APDT. In addition, Caminos *et al.* showed that, in porphyrins with cationic (A) and non-cationic (B) groups, the photosensitized inactivation of *E. coli* cellular suspensions with those compounds follows the order:  $A_3B^{3+} > A_4^{4+} \gg ABAB^{2+} > AB_3^{+}$ .<sup>23</sup>

In this paper, we report the synthesis of the first aryl cationic water-soluble porphycene as well as its photochemical characterization. In addition, we herein present the results of a study designed to evaluate *in vitro* the broad-spectrum antimicrobial efficacy of this novel light-activated PS against a panel of prototypical human pathogenic microbes, as well as its potential *in vivo* application to infection using a 3<sup>rd</sup> degree mouse burn model infected with a drug-resistant bacterial strain, methicillin-resistant *Staphylococcus aureus* (MRSA).

## Experimental section

### Reagents and solvents

2,7,12,17-tetrakis-(*p*-(methoxymethyl)phenyl) porphycene (**1**; MeO<sub>4</sub>-TBPO) was prepared using previously described procedures.<sup>14</sup> All other reagents were purchased from Sigma-Aldrich and were used as received: HBr (33 wt. % in acetic acid); pyridine (ACS reagent, ≥99.0%). Solvents used for spectroscopic measurements were spectrophotometric grade.

### Chemical synthesis

Nuclear magnetic resonance spectra were obtained with a Varian Gemini 400HC (400 MHz <sup>1</sup>H-NMR and 100.5 MHz <sup>13</sup>C-NMR) equipment. Chemical shifts are expressed in ppm. For the <sup>1</sup>H-NMR spectra, trimethylsilane (TMS) was used as reference. For the <sup>13</sup>C-NMR spectra, the chemical shifts of the solvents (d<sub>6</sub>-DMSO and CDCl<sub>3</sub>) were used as standards. The notation for the analysis is: s (singlet), d (doublet), t (triplet), q (quartet), dd (doublet of doublets), m (multiplet), sd (deuterable signal), brs. (broad signal). High resolution mass spectra (HRMS) were registered with a Microtof (Bruker) of high resolution (ESI-TOF technique) by the mass spectroscopy service of Universidade de Santiago de Compostela.

### 2,7,12-tris(*p*-(bromomethyl)phenyl)-17-(*p*-(methoxymethyl)phenyl) porphycene (**2**; Br<sub>3</sub>MeO-TBPO)

204 mg (0.26mmol) of MeO<sub>4</sub>-TBPO were dissolved in 200 mL of anhydrous dichloromethane. Then, 43 mL of hydrogen bromide solution 33 wt. % in acetic acid (425 mmol) were added drop wise while standing the system in a water / ice bath 3 h. Finally, the reaction mixture was diluted with 200 mL of chilled water and the organic phase was extracted with dichloromethane. The organic layer was washed with water and NaHCO<sub>3</sub> saturated solution. The organic extracts were dried over MgSO<sub>4</sub> and solvent removed under reduced pressure. The raw brominated mixture was purified through a silica pad (cyclohexane/dichloromethane; 1:1) and the desired product, that elutes the second, is isolated and washed with cyclohexane. 25 mg of product **2** (η = 10%) were obtained as dark violet powder. <sup>1</sup>H-NMR (δ / ppm, CDCl<sub>3</sub>): 9.93 (s, 1H), 9.92 (s, 3H), 9.70 (s, 4H), 8.32 (d, *J*

= 8.0 Hz, 8H), 7.85 (d,  $J$  = 8.0 Hz, 8H), 7.80 (d, 2H), 4.79 (s, 6H), 4.75 (s, 2H); 3.58 (s, 3H).  $^{13}\text{C}$ -NMR ( $\delta$  / ppm,  $\text{CDCl}_3$ ): 137.6, 136.8, 132.1, 132.0, 131.6, 131.5, 129.9, 129.4, 128.6, 74.8, 33.7, 29.9. UV/Vis (Toluene): 666 (46060), 631 (47100), 588 (34630), 396 (82680), 380 (102100). HRMS (ESI-TOF)  $m/z$   $\text{C}_{49}\text{H}_{37}\text{Br}_3\text{N}_4\text{O}$  calcd, 937.0550; found, 937.0578

### 2,7,12-tris( $\alpha$ -pyridinio-*p*-tolyl)-17-(*p*-(methoxymethyl)phenyl) porphycene (**3**, $\text{Py}_3\text{MeO-TBPo}$ )

25 mg of tribrominated  $\text{Br}_3\text{MeO-TBPo}$  were placed in a 50mL round bottom flask and dissolved with the minimum amount of pyridine. The solution was heated at 80 °C for 2 h and the precipitated solid recovered after centrifugation. The solid was washed with *tert*-butyl methyl ether (3×5mL) and dried under vacuum. 25mg of product **3** were obtained as a dark powder ( $\eta$  = 85%). Purity of **3** was confirmed by thin layer chromatography using a pre-coated TLC plate (Silica gel C18 0.25mm; Macherey-Nagel) in a trifluoroacetic acid/ acetonitrile mixture (20:80), providing a unique spot at  $R_f$  = 0.26, and by HPLC analysis using a Lichrocart Purospher STAR RP-18E column (see Supporting Information).  $^1\text{H}$ -NMR ( $\delta$  / ppm,  $d_6$ -DMSO): 10.19 (brs, 4H), 10.05 (brs, 4H), 9.47 (d,  $J$  = 9.2 Hz, 6H), 8.76 (t, 3H), 8.50 (d, 6H), 8.40 (d,  $J$  = 8.0Hz, 2H), 8.34 (t, 6H), 8.06 (d,  $J$  = 9.2 Hz, 6H), 7.84 (d,  $J$  = 8.0 Hz, 2H), 3.83 (t, 2H), 8.06 (d,  $J$  = 9.2 Hz, 12H); 6.18 (s, 6H), 4.72 (s, 2H), 3.83 (s, 2H), 3.49 (s, 3H).  $^{13}\text{C}$ -NMR ( $\delta$  / ppm,  $d_6$ -DMSO): 146.7, 145.5, 144.7, 144.1, 143.8, 143.5, 142.7, 142.4, 142.0, 138.9, 137.0, 135.0, 134.8, 134.5, 134.1, 132.4, 131.6, 130.3, 129.1, 128.9, 125.9, 115.3, 73.9, 63.6, 58.3. UV/Vis (MeOH): 656 (112200), 624 (99890), 582 (80850), 391 (190700), 375 (232400). HRMS (ESI-TOF)  $m/z$   $\text{C}_{52}\text{H}_{47}\text{N}_4\text{O}_4^{2+}$  calcd, 466.7072; found, 466.7066.

### General spectroscopic measurements

Absorption spectra were recorded on a Cary 4E spectrophotometer (Varian, Palo Alto, CA). Absorption coefficients were derived from the slopes of Beer-Lambert plots. Fluorescence emission spectra were recorded in a Spex Fluoromax-2 spectrofluorometer (Horiba Jobin-Yvon, Edison, NJ). Fluorescence decays were recorded with a time-correlated single photon counting system (Fluotime 200, PicoQuant GmbH, Berlin, Germany) equipped with a red sensitive photomultiplier. Excitation was achieved by means of a 375 nm picosecond diode laser working at 10 MHz repetition rate. The counting frequency was always below 1%. Fluorescence lifetimes were analyzed using PicoQuant FluoFit 4.0 data analysis software. Transient absorption spectra were monitored by nanosecond laser flash photolysis using a Q-switched Nd-YAG laser (Surelite I-10, Continuum) with right-angle geometry and an analysing beam produced by a Xe lamp (PTI, 75 W) in combination with a dual-grating monochromator (mod. 101, PTI) coupled to a photomultiplier (Hamamatsu R928). Kinetic analysis of the individual transients was performed with software developed in our laboratory.

$^1\text{O}_2$  phosphorescence was detected by means of a customized PicoQuant Fluotime 200 system described in detail elsewhere.<sup>24</sup>  $^1\text{O}_2$  signal amplitudes were determined by analysis of the data using the FluoFit 4.0 software.

All spectroscopic measurements were carried out in 1-cm quartz cuvettes (Hellma, Germany) at room temperature.

### Microbial Strains and Culture Conditions

The microorganisms studied were *Staphylococcus aureus* 8325-4, methicilin-resistant *S. aureus* Xen 31 (a kind gift from Xenogen Corp, Alameda, CA) and *Enterococcus faecalis* (ATCC29212) as Gram-positive bacteria; *Acinetobacter baumannii* (ATCC 51393),

*Escherichia coli* (ATCC 53868), *Proteus mirabilis* (ATCC 51393) and *Pseudomonas aeruginosa* (ATCC 19660) as Gram-negative bacteria; and *Candida albicans* (ATCC 18804) and *C. krusei* (ATCC 6258) as yeasts.

Bacteria were aerobically grown overnight at 37°C in an orbital shaking incubator at 130 rpm in brain-heart infusion (BHI) broth (Fischer Scientific) to stationary phase, and an aliquot was then grown in fresh BHI medium at 37°C to an  $Abs_{600} = 0.5$ , corresponding to *ca.*  $10^8$  colony forming units (CFU)/mL (logarithmic phase). The suspensions were then centrifuged (5 min, 3500 rpm) and resuspended with sterile PBS at pH 7.4 at the same concentration for phototoxicity experiments. *C. albicans* was grown overnight at 30°C in yeast peptone dextrose (YPD) broth (Fischer Scientific), centrifuged (5 min, 3500 rpm) and resuspended with sterile PBS at pH 7.4 up to *ca.*  $10^7$  CFU/mL for phototoxicity experiments. *C. krusei* was grown overnight at 35 °C in Sabouraud broth (Merck), and then grown in new Sabouraud medium at 35°C in an orbital shaking incubator at 130 rpm to an  $Abs_{600} = 0.7$ , corresponding to *ca.*  $10^7$  CFU/mL. The suspensions were then centrifuged (5 min, 3500 rpm) and resuspended with sterile PBS at pH 7.4 at the same concentration for phototoxicity experiments.

### Light sources

All bacterial suspensions and *C. albicans* were irradiated with a  $652 \pm 15$  nm light delivered by a non-coherent light source (LumaCare, Newport Beach, CA), an optical fiber bundle, and a lens (to form a 2-cm diameter spot) using a  $125 \text{ mW} \cdot \text{cm}^{-2}$  fluence rate. *C. krusei* was irradiated by means of a Sorisa Photocare at  $635 \pm 10$  nm using a  $35 \text{ mW} \cdot \text{cm}^{-2}$  fluence rate.

Fluence rates were routinely measured using a power meter (Coherent, Portland, OR).

### Photodynamic inactivation studies

Suspensions of bacteria ( $10^8$  CFU/mL) or yeast ( $10^7$  CFU/mL) in PBS were incubated in the dark at room temperature for 30 min with increasing concentrations of the PS (added from 5mM dimethylacetamide (DMA) stock solution). Centrifugation (3 min, 12000 rpm) of 1-mL aliquots was used to remove the excess of PS that was not taken up by the microbial cells when experiments required it. Then 1-mL aliquots of the cells suspensions were placed in 24-well plates. The wells were illuminated from the top of the plates by use of red light and fluences ranged from 0 to  $100 \text{ J} \cdot \text{cm}^{-2}$ . At times during the illumination when the requisite fluences had been delivered, aliquots were taken from each well (the suspensions were thoroughly mixed before sampling to avoid the settlement of bacteria). For determination of CFU, the aliquot was serially diluted, streaked on nutrient agar and incubated in the dark for 18 h at 37°C or 30°C. Experiments were carried out in triplicate for each condition. Controls using the same amount of organic solvent, in the presence of the porphycene and without light, and with light alone were performed for all experimental conditions, obtaining less than  $1\text{-log}_{10}$  reduction in bacterial viability in all cases.

### Photodynamic inactivation in a burn infected mouse model

Adult female BALB/c mice (Charles River Laboratories, Wilmington, MA), 6-8 week old and weighing 17-21 g, were used in the study. The animals were housed one per cage and maintained on a 12-hour light/dark cycle with access to food and water *ad libitum*. All animal procedures were approved by the Subcommittee on Research Animal Care (IACUC) of Massachusetts General Hospital and met the guidelines of National Institutes of Health. Twenty mice were randomly divided into four groups of five animals each; these groups were designated (A) PDT; (B) PS dark control; (C) light alone control; (D) no treatment control. *In vivo* experiments were performed in burn infections by means of the protocol used by Dai *et al.* fully described elsewhere.<sup>25</sup> Briefly, bacterial infection took place as

described by Ha *et al.*<sup>26</sup> Five minutes after the creation of burns (to allow the burns to cool down), a suspension (50  $\mu\text{L}$ ) of bacteria in sterile PBS containing  $10^8$  cells was inoculated onto the surface of each burn with a pipette tip and then was smeared onto the burn surface with an inoculating loop. The bioluminescence imaging system (Hamamatsu Photonics KK, Bridgewater, NJ) has been described elsewhere in detail.<sup>27</sup> Briefly, an ICCD photon-counting camera (Model C2400-30H; Hamamatsu Photonics, Bridgewater, NJ) was used. The camera was mounted in a light-tight specimen chamber, fitted with a light-emitting diode, a set-up that allowed for a background gray-scale image of the entire mouse to be captured. By accumulating many images containing binary photon information (an integration time of 2 minutes was used), a pseudo-color luminescence image was generated. Superimposition of this image onto the gray-scale background image yielded information on the location and intensity in terms of photon number. The camera was also connected to a computer system through an image processor (Argus-50, Hamamatsu Photonics). Argus-50 control program (Hamamatsu Photonics) was used to acquire images and to process the image data collected. The mice were imaged immediately after applying the bacteria to ensure that the bacterial inoculum applied to each burn was consistent.

Thirty minutes after the infection, 50  $\mu\text{L}$  of porphycene solution (10% dimethylsulfoxide in PBS) were added to groups A and B and 30 minutes was allowed for the PS to bind to and penetrate the bacteria. Then, mice were again imaged to quantify any dark toxicity to the bacteria. Mice (groups A and C) were then illuminated with  $652 \pm 15$  nm light delivered by a non-coherent light source with a power density of  $100 \text{ mW}\cdot\text{cm}^{-2}$ . Mice were given total light doses of  $180 \text{ J}\cdot\text{cm}^{-2}$  in aliquots with bioluminescence imaging taking place after each aliquot of light. Immediately after PDT, mice in all groups were resuscitated with an IP injection of 0.5 mL sterile saline to prevent dehydration.

## Statistics

Survival fractions are expressed as means  $\pm$  standard error of the mean (SEM) of three independent experiments. Differences between the killing curves were evaluated by means of paired Student's *t* test. Differences between three or more means were compared by a one-way ANOVA. *P* values of  $< 0.05$  were considered as significant.

## Results

### Synthesis

Treatment of porphycene **1** with HBr (33% in acetic acid) in dichloromethane<sup>27</sup> furnishes a mixture of brominated porphycenes resulting from the substitution of methoxy groups with bromine atoms at the benzylic positions. From this mixture, mainly inseparable dibrominated derivatives, the tribrominated porphycene **2** can be isolated easily by column chromatography. Finally, heating of porphycene **2** in pyridine as a solvent provides the corresponding pure tribromide **3** ( $\text{Py}_3\text{MeO-TBPO}\cdot\text{Br}_3$ )<sup>28, 29</sup> as a deep blue precipitate. Purity of **3** was determined by multiple methods including (low-resolution) laser desorption mass spectrometry, (high-resolution) electrospray mass spectrometry,  $^1\text{H}$  and  $^{13}\text{C}$  NMR spectroscopy, UV-Visible absorption spectroscopy, fluorescence spectroscopy, HPLC analysis, and reverse phase thin-layer chromatography (see Supporting Information). In all cases the purity was estimated to be  $> 95\%$ .

### Physical and photophysical properties

The photophysical properties of  $\text{Py}_3\text{MeO-TBPO}$  are summarized in Table 1. As observed in Figure 1,  $\text{Py}_3\text{MeO-TBPO}$  shows the typical porphycene absorption spectrum in MeOH, with three bands in the red range of the spectrum and absorption coefficients in the  $50,000 \text{ M}^{-1} \text{ cm}^{-1}$  range. The spectrum in water loses much of the structure, indicating not surprisingly

that aggregation is occurring in aqueous media despite the three positive charges. The extent of aggregation can be controlled by changing the ionic strength of the solution, i.e., the compound is substantially more aggregated in PBS than in pure water. However, both in aqueous solvents and in MeOH the fluorescence emission spectra match the typical fluorescence spectrum of porphycenes, where a main band and a weaker shoulder at lower energies are observed that are the mirror image of the  $S_1 \leftarrow S_0$ -absorption transition<sup>11</sup> Interestingly, the fluorescence excitation spectrum matches in all cases the absorption spectrum of the monomer, indicating that the aggregates are not emissive.

The fluorescence quantum yield,  $\Phi_F$ , was determined by comparing the integrated fluorescence intensity of the porphycene to that of an optically-matched solution of cresyl violet in MeOH as reference ( $\Phi_F = 0.54$ )<sup>30</sup>. A value of  $\Phi_F = 0.075 \pm 0.005$  was found in MeOH, while in water the results showed a marked dependence on the excitation wavelength, reflecting the fraction of monomers that were excited at each wavelength (see Supporting Information). The fluorescence decay was monoexponential in both solvents (Figure 1B and 1D), with lifetimes  $1.8 \pm 0.1$  ns in water and  $2.6 \pm 0.1$  ns in MeOH. This is consistent with the similar excitation spectra and confirms that only the monomers are emissive.

Transient absorption spectra of  $\text{Py}_3\text{MeO-TBPO}$  in argon atmosphere are shown in Figure 2. Again, they present a shape similar to that of the triplet-minus-singlet spectrum of tetraphenylporphycene (TPPo), confirming that only the monomeric species can undergo intersystem crossing.<sup>31</sup> The decays at 420 nm show a triplet lifetime of 330  $\mu\text{s}$  in water and 152  $\mu\text{s}$  in MeOH, with rate constants of oxygen quenching ( $k_q$ ) of  $1.5 \times 10^9 \text{ M}^{-1}\cdot\text{s}^{-1}$  and  $3.5 \times 10^9 \text{ M}^{-1}\cdot\text{s}^{-1}$ , respectively.

The singlet oxygen ( $^1\text{O}_2$ ) production quantum yield,  $\Phi_\Delta$ , was determined by means of its phosphorescence at 1270 nm (Figure 2B), comparing the intensity of the  $^1\text{O}_2$  signal shown by the porphycene to that of optically-matched solutions of reference PSs.<sup>32</sup> Using *m*-tetrahydroxyphenylporphine (*m*-THPP) and tetra-*N*-methylpyridylporphine (TMPyP) as standards ( $\Phi_\Delta^{\text{ref}} = 0.69$  and  $0.74$ , respectively),<sup>33, 34</sup>  $\Phi_\Delta$  values of  $0.004 \pm 0.001$  and  $0.19 \pm 0.01$  were determined in water and MeOH, respectively, upon excitation at 532 nm. While in MeOH the  $\Phi_\Delta$  values were independent of the excitation wavelength, we obtained  $\Phi_\Delta = 0.03 \pm 0.01$  in water upon excitation at 355 nm using sulfonated phenalenone as standard ( $\Phi_\Delta^{\text{ref}} \sim 1$ ).<sup>35</sup> It can thus be concluded that the photophysical properties of **3** in MeOH are very similar to those of typical tetraphenylporphycenes,<sup>11</sup> while in aqueous media aggregation strongly prevents its photosensitizing ability. This finding is fully in line with the results of decades of research on related tetrapyrrole macrocycles.

### ***In vitro* photoinactivation of bacteria**

All Gram-positive tested species were completely eliminated (no colonies observed) by PDT in a porphycene-concentration (Figure 3A) and energy-dose (see Supporting Information) dependent manner. *E. faecalis* was the most sensitive species to  $\text{Py}_3\text{MeO-TBPO-PDT}$  showing 6- $\log_{10}$  reduction in bacterial viability with a 0.5  $\mu\text{M}$  porphycene concentration and an energy dose of 30  $\text{J}\cdot\text{cm}^{-2}$ . 1  $\mu\text{M}$  or 2  $\mu\text{M}$  porphycene concentration and 15  $\text{J}\cdot\text{cm}^{-2}$  were needed respectively to produce a similar effect for *S. aureus* and MRSA in a porphycene-concentration and energy-dose dependent manner.

Gram-negative species could be similarly inactivated (Figure 3B and Supporting Information), although higher concentrations and light doses were needed. For instance, 8  $\mu\text{M}$  of **3** and 100  $\text{J}\cdot\text{cm}^{-2}$  were needed to induce a 6- $\log_{10}$  reduction in the bacterial viability for *A. baumannii*, while 10  $\mu\text{M}$  and 60  $\text{J}\cdot\text{cm}^{-2}$  were needed in the case of *E. coli*. Only a modest 3- $\log_{10}$  reduction in the survival fraction was achieved for *P. mirabilis* even at 50

$\mu\text{M}$  and  $100 \text{ J}\cdot\text{cm}^{-2}$ , and no relevant inactivation ( $< 1\text{-log}_{10}$  reduction in the survival fraction) could be observed for *P. aeruginosa* even at  $100 \mu\text{M}$  porphycene-concentration and light dose of  $100 \text{ J}\cdot\text{cm}^{-2}$ .

All the inactivation curves were performed with and without removing the excess of PS (Figures 3C and 3D). No significant statistical difference was obtained in any case ( $P > 0.26$ ). This finding implied that the porphycene displayed strong binding to the bacterial cells.

### ***In vitro* photoinactivation of yeasts**

*Candida* species are generally used in APDT as representative models of fungal cells as they grow as single cell suspensions. Both species were completely eliminated by  $\text{Py}_3\text{MeO-TBPO}$  in a concentration (Figure 4) and light-dose dependent manner (see Supporting Information), irrespective of the removal or not of the porphycene excess from the solution. As observed in figure, while  $50 \mu\text{M}$  concentration of  $\text{Py}_3\text{MeO-TBPO}$  and  $30 \text{ J}\cdot\text{cm}^{-2}$  were needed to obtain a  $5\text{-log}_{10}$  reduction in the cell viability of *C. albicans*, only  $10 \mu\text{M}$  concentration and  $15 \text{ J}\cdot\text{cm}^{-2}$  proved necessary to produce the same reduction in the cell viability of *C. krusei*. Removing the excess of PS did not produce any significant difference ( $P = 0.75$ ).

### ***In vivo* photoinactivation of MRSA in infected burns**

Bioluminescent MRSA (Xen31) has a stably integrated lux operon that has been optimized for expression in Gram-positive bacteria<sup>36</sup> and leads to spontaneous light emission at  $37^\circ\text{C}$  in the absence of any exogenously added substrate. It has been previously demonstrated that MRSA CFUs quantified using serial dilutions of bacterial suspensions correlate linearly with the bioluminescence emitted by those bacteria.<sup>36</sup>

Figure 5A shows the successive bioluminescence images obtained from four representative mouse burns (from groups A, B, C, and D) infected with MRSA. The burn treated with PDT received  $100 \mu\text{M}$  of  $\text{Py}_3\text{MeO-TBPO}$  and  $652 \text{ nm}$  light up to  $180 \text{ J}\cdot\text{cm}^{-2}$ , the dark control burn, received the same amount of porphycene and no light; while the light alone burn received  $652 \text{ nm}$  light up to  $180 \text{ J}\cdot\text{cm}^{-2}$  and no porphycene. A non-treated control burn, received neither PS nor light. A complete elimination of the bioluminescence signal was observed in the PDT treated burn after a light dose of  $180 \text{ J}\cdot\text{cm}^{-2}$  in the presence of  $\text{Py}_3\text{MeO-TBPO}$ .

The light-dose responses of normalized mean bioluminescence values ( $n=5$ ) of the different mouse groups are shown in figure 5B. PDT induced a reduction of  $ca. 2.6\text{-log}_{10}$  of the bioluminescence while less than  $0.3\text{-log}_{10}$  reduction was observed for all the control groups. The statistical analysis at each energy-dose by 1-factor ANOVA test showed significant differences among all the control groups and the PDT-treated group ( $P < 0.001$ ).

## **Discussion**

A potential PS for APDT must have appropriate photophysical properties, such as a large long wavelength absorption band and a high quantum yield for the generation of both long-lived triplet excited state and cytotoxic ROS species. It also has to be water soluble and must have a high affinity for microbial cells and a low affinity for host cells; characteristics that are strongly related to the presence of cationic charges in the molecular structure.

As observed in the absorption spectrum and despite the cationic charges,  $\text{Py}_3\text{MeO-TBPO}$  is soluble although aggregated in water, which deteriorates its photophysical properties. The differential behavior in aqueous and more lipophilic environments may be valuable for unmistakably ascertaining the localization of the porphycene bound to the cells by means of

fluorescence microscopy. From the point of view of APDT applications, it can be expected that Py<sub>3</sub>MeO-TBPO would be a good PS if binding to microbial cells prevents its aggregation. Conversely, any non-bound PS will be aggregated and thus will not be able to cause photodamage to surrounding tissue. The fact that the absorption spectrum of the aggregates shows lower absorption coefficients is also an advantage as these non-bound molecules will see their light-filtering ability reduced. The presence of aggregates can also be observed in the  $\Phi_F$  and  $\Phi_\Delta$  values in water. For instance, as observed in Table 1, the  $\Phi_\Delta$  drops from 0.03 to 0.004 when changing the excitation wavelength. This change is due to the different absorption coefficient ratio monomer/aggregates at both wavelengths. At 355 nm, the ratio is higher, leading to a lower light-filtering effect, *i.e.*, to a higher  $\Phi_\Delta$ . The different trend observed in the lifetime values of the singlet ( $\tau_s$ ) and triplet ( $\tau_T$ ) excited states can be explained by two different factors. On one hand, the presence of aggregates in H<sub>2</sub>O enables a new deactivation pathway by intermolecular interactions of the porphycene molecules, leading to a decrease in the  $\tau_s$  value. Compared to TPPo ( $\tau_T = 4.8$  ns in toluene), <sup>37</sup>  $\tau_s$  in MeOH is lower probably due to the higher freedom degree of the residues bound to the porphycene ring. On the other hand, the triplet excited state population is basically controlled by the oxygen concentration in the solutions ( $k_q \sim 10^9$  M<sup>-1</sup>s<sup>-1</sup>). Thus, despite the measurements having been performed in argon-saturated solutions, the solubility of oxygen in H<sub>2</sub>O is lower than in MeOH, *i.e.*, the remaining amount of oxygen molecules in the solutions is lower, leading then to a longer  $\tau_T$  value. As regards  $k_q$ , the values are in the range of those observed in diffusional controlled quenching reactions, and the reduction observed in H<sub>2</sub>O, relative to that in MeOH, is due to the higher viscosity of water.

Concerning the *in vitro* PDT experiments with Gram-positive bacteria, it was observed that low concentrations of porphycene (< 2  $\mu$ M), as well as low light doses (< 30 J·cm<sup>-2</sup>) were enough to completely eliminate all the strains. On the other hand, because of the generally higher resistance of Gram-negative species,<sup>16</sup> higher light doses (> 60 J·cm<sup>-2</sup>) were needed in order to inactivate the Gram-negative bacterial strains tested with somewhat larger PS concentrations (< 10  $\mu$ M). However, neither high concentrations of porphycene nor high light doses were able to completely eliminate *P. mirabilis* or significantly inactivate *P. aeruginosa*. A possible reason for the different susceptibility within Gram-positive bacterial strains is the difference in anti-oxidant enzyme levels. As for Gram-negative bacteria, a possible explanation can be the different membrane permeability between *A. baumannii* (high), *E. coli* (intermediate) and *P. mirabilis* (low).

Consistent with the photophysics results there are no significant differences between the inactivation curves recorded in the presence or absence of the excess PS ( $P > 0.26$ ), suggesting a high lipophilicity of the porphycene, *i.e.*, a high affinity against bacterial cells, which indicates that only the PS bound to the cells is involved in the photodynamic effect. Thus, according to the classification of PSs established by Deminova and Hamblin,<sup>17</sup> the porphycene might be tightly bound to the microbial cell and might be able to penetrate into microorganisms, as happened when poly-L-lysine chlorin(e6) conjugate was used as PS.

As for the yeast studies, *Candida* species were selected as model to study the activity of porphycenes against fungal cells. Our data show that porphycenes can be used as a valuable alternative to typical anti-fungal PSs, as they are able to completely inactivate both *C. albicans* and *C. krusei* using lower light doses and lower porphycene concentrations than for currently-used PSs.<sup>17, 38-40</sup>

Despite the optimal properties of the porphycene *in vitro*, its value as PS must be further assessed from experiments *in vivo*.

DMA was used as *in vitro* stock solution because it does not quench hydroxyl radicals. However, PBS with DMSO was used as *in vivo* stock solution instead of DMA because DMSO helps the penetration of the dye into the infected tissue. The test in burns infected with MRSA demonstrate that porphycenes can clearly produce statistically significant differences between the controls and the PDT-treated group ( $P < 0.001$ ), reducing by 2.6- $\log_{10}$  units the bioluminescence of MRSA in an energy-dose dependent manner upon irradiation with 180 J·cm<sup>-2</sup> and a porphycene concentration of 100  $\mu$ M. These results compare favorably to those obtained by Dai *et al.*,<sup>41</sup> where a 2.7- $\log_{10}$  reduction of the bioluminescence signal was obtained in a skin abrasion wound infected with MRSA by using polyethylenimine-chlorin(e6) conjugate and 660-nm red light, and by Zolfaghari *et al.*,<sup>42</sup> where 1.4- $\log_{10}$  and 1.15- $\log_{10}$  were obtained in excision and superficial scarified wounds treated with methylene blue and 670-nm red light, respectively.

## Conclusions

The synthetic availability of cationic porphycenes, as well as their optimal physical and photophysical properties, suggests the porphycene-core macrocycle can be a potentially interesting antimicrobial PS. The demonstrated high photodynamic activity against a broad-spectrum of microbial cells *in vitro* as well as an *in vivo* infection model, supports the further scrutiny of this family of compounds.

## Supplementary Material

Refer to Web version on PubMed Central for supplementary material.

## Acknowledgments

This work was supported by a grant of the Spanish Ministerio de Ciencia e Innovación (CTQ2007-67763-C03-01/BQU) and by US NIH grant R01AI050875 to MRH. X.R. and R.R. were supported by the Generalitat de Catalunya (DURSI) and Fons Social Europeu with a predoctoral fellowship. R.R. also thanks Obra Social “la Caixa” for its Master’s grant. T.D. was supported by the Bullock-Wellman Postdoctoral Fellowship Award. We thank Sorisa<sup>®</sup> for providing us with the Sorisa Photocare LED source and Xenogen Corp for the gift of XEN31.

## References

1. Wainwright M. Photodynamic antimicrobial chemotherapy (PACT). *J Antimicrob Chemother.* 1998; 42:13–28. [PubMed: 9700525]
2. Wainwright M. Photoantimicrobials--so what's stopping us? *Photodiagn Photodyn Ther.* 2009; 6:167–169.
3. Dai T, Huang YY, Hamblin MR. Photodynamic therapy for localized infections--state of the art. *Photodiagn Photodyn Ther.* 2009; 6:170–188.
4. Schweitzer C, Schmidt R. Physical mechanisms of generation and deactivation of singlet oxygen. *Chem Rev.* 2003; 103:1685–1757. [PubMed: 12744692]
5. Michaeli A, Feitelson J. Reactivity of singlet oxygen toward amino acids and peptides. *Photochem Photobiol.* 1994; 59(3):284–289. [PubMed: 8016206]
6. Stark G. Functional consequences of oxidative membrane damage. *J Membr Biol.* 2005; 205:1–16. [PubMed: 16245038]
7. Ravanat JL, Di Mascio P, Martinez GR, Medeiros MHG, Cadet J. Singlet oxygen induces oxidation of cellular DNA. *J Biol Chem.* 2000; 275:40601–40604. [PubMed: 11007783]
8. Nitzan Y, Gutterman M, Malik Z, Ehrenberg B. Inactivation of Gram-Negative Bacteria by Photosensitized Porphyrins. *Photochem Photobiol.* 1992; 55:89–96. [PubMed: 1534909]
9. Bertoloni G, Rossi F, Valduga G, Jori G, Ali H, Vanlier JE. Photosensitizing activity of water-soluble and lipid-soluble phthalocyanines on prokaryotic and eukaryotic microbial-cells. *Microbios.* 1992; 71:33–46. [PubMed: 1406343]

10. Romanova NA, Brovko LY, Moore L, Pometun E, Savitsky AP, Ugarova NN, Griffiths MW. Assessment of photodynamic destruction of *Escherichia coli* O157 : H7 and *Listeria monocytogenes* by using ATP bioluminescence. *Appl Environ Microbiol.* 2003; 69:6393–6398. [PubMed: 14602591]
11. Stockert JC, Canete M, Juarranz A, Villanueva A, Horobin RW, Borrell J, Teixido J, Nonell S. Porphycenes: Facts and prospects in photodynamic therapy of cancer. *Curr Med Chem.* 2007; 14:997–1026. [PubMed: 17439399]
12. Polo L, Segalla A, Bertoloni G, Jori G, Schaffner K, Reddi E. Polylysine-porphycene conjugates as efficient photosensitizers for the inactivation of microbial pathogens. *J Photochem Photobiol B:Biol.* 2000; 59:152–158.
13. Lauro FM, Pretto P, Covolo L, Jori G, Bertoloni G. Photoinactivation of bacterial strains involved in periodontal diseases sensitized by porphycene-polylysine conjugates. *Photochem Photobiol Sci.* 2002; 1:468–470. [PubMed: 12659156]
14. Sanchez-Garcia D, Borrell JI, Nonell S. One-pot synthesis of substituted 2,2' - bipyrrroles. A straightforward route to aryl porphycenes. *Org Lett.* 2009; 11:77–79. [PubMed: 19053828]
15. Bertoloni G, Rossi F, Valduga G, Jori G, Vanlier J. Photosensitizing activity of water-soluble and lipid-soluble phthalocyanines on *Escherichia coli*. *FEMS Microbiol Lett.* 1990; 71:149–155. [PubMed: 2125956]
16. Malik Z, Ladan H, Nitzan Y. Photodynamic inactivation of gram-negative bacteria - Problems and possible solutions. *J Photochem Photobiol B:Biol.* 1992; 14:262–266.
17. Demidova TN, Hamblin MR. Effect of cell-photo sensitizer binding and cell density on microbial photoinactivation. *Antimicrob Agents Chemother.* 2005; 49:2329–2335. [PubMed: 15917529]
18. Guo YY, Rogelj S, Zhang P. Rose bengal-decorated silica nanoparticles as photosensitizers for inactivation of gram-positive bacteria. *Nanotechnology.* 2010; 21
19. Friedberg JS, Tompkins RG, Rakestraw SL, Warren SW, Fischman AJ, Yarmush ML. Antibody-targeted photolysis - bacteriocidal effects of Sn (IV) chlorin e6- Dextran-monoclonal antibody conjugates. *Ann NY Acad Sci.* 1991; 618:383–393. [PubMed: 1706578]
20. Minnock A, Vernon DI, Schofield J, Griffiths J, Parish JH, Brown SB. Photoinactivation of bacteria. Use of a cationic water-soluble zinc phthalocyanine to photoinactivate both gram-negative and gram-positive bacteria. *J Photochem Photobiol B:Biol.* 1996; 32:159–164.
21. Merchat M, Bertolini G, Giacomini P, Villanueva A, Jori G. Meso-substituted cationic porphyrins as efficient photosensitizers of gram-positive and gram-negative bacteria. *J Photochem Photobiol B:Biol.* 1996; 32:153–157.
22. Wainwright M, Phoenix DA, Marland J, Wareing DRA, Bolton FJ. A study of photobactericidal activity in the phenothiazinium series. *FEMS Immunol Med Microbiol.* 1997; 19:75–80. [PubMed: 9322071]
23. Caminos DA, Spesia MB, Durantini EN. Photodynamic inactivation of *Escherichia coli* by novel meso-substituted porphyrins by 4-(3-*N,N,N*-trimethylammoniumpropoxy)phenyl and 4-(trifluoromethyl)phenyl groups. *Photochem Photobiol Sci.* 2006; 5:56–65. [PubMed: 16395428]
24. Jimenez-Banzo A, Ragas X, Kapusta P, Nonell S. Time-resolved methods in biophysics. 7. Photon counting vs. analog time-resolved singlet oxygen phosphorescence detection. *Photochem Photobiol Sci.* 2008; 7:1003–1010. [PubMed: 18754045]
25. Dai TH, Tegos GP, Lu ZS, Huang LY, Zhiyentayev T, Franklin MJ, Baer DG, Hamblin MR. Photodynamic therapy for *Acinetobacter baumannii* burn infections in mice. *Antimicrob Agents Chemother.* 2009; 53:3929–3934. [PubMed: 19564369]
26. Ha UW, Jin SG. Expression of the *soxR* gene of *Pseudomonas aeruginosa* is inducible during infection of burn wounds in mice and is required to cause efficient bacteremia. *Infect Immun.* 1999; 67:5324–5331. [PubMed: 10496912]
27. Hamblin MR, O'Donnell DA, Murthy N, Contag CH, Hasan T. Rapid control of wound infections by targeted photodynamic therapy monitored by in vivo bioluminescence imaging. *Photochem Photobiol.* 2002; 75:51–57. [PubMed: 11837327]
28. Yamashita T, Uno T, Ishikawa Y. Stabilization of guanine quadruplex DNA by the binding of porphyrins with cationic side arms. *Bioorg Med Chem.* 2005; 13:2423–2430. [PubMed: 15755644]

29. Ikawa Y, Moriyama S, Harada H, Furuta H. Acid-base properties and DNA-binding of water soluble *N*-confused porphyrins with cationic side-arms. *Org Biomol Chem*. 2008; 6:4157–4166. [PubMed: 18972046]
30. Magde D, Brannon JH, Cremers TL, Olmsted J. Absolute luminescence yield of cresyl violet - Standard for the red. *J Phys Chem*. 1979; 83:696–699.
31. Rubio N, Borrell JI, Teixido J, Canete M, Juarranz A, Villanueva A, Stockert JC, Nonell S. Photochemical production and characterisation of the radical ions of tetraphenylporphycenes. *Photochem Photobiol Sci*. 2006; 5:376–380. [PubMed: 16583017]
32. Nonell, S.; Braslavsky, SE. *Methods in Enzymology*. Academic Press; 2000. p. 1-682.
33. Wilkinson F, Helman WP, Ross AB. Quantum yields for the photosensitized formation of the lowest electronically excited singlet state of molecular oxygen in solution. *J Phys Chem Ref Data*. 1993; 22:113–262.
34. Redmond RW, Gamlin JN. A compilation of singlet oxygen yields from biologically relevant molecules. *Photochem Photobiol*. 1999; 70:391–475. [PubMed: 10546544]
35. Nonell S, Gonzalez M, Trull FR. 1*H*-Phenalen-1-One-2-Sulfonic Acid - An extremely efficient singlet molecular-oxygen sensitizer for aqueous-media. *Afinidad*. 1993; 50:445–450.
36. Francis KP, Joh D, Bellinger-Kawahara C, Hawkinson MJ, Purchio TF, Contag PR. Monitoring bioluminescent *Staphylococcus aureus* infections in living mice using a novel luxABCDE construct. *Infect Immun*. 2000; 68:3594–3600. [PubMed: 10816517]
37. Rubio N, Prat F, Bou N, Borrell JI, Teixido J, Villanueva A, Juarranz A, Canete M, Stockert JC, Nonell S. A comparison between the photophysical and photosensitising properties of tetraphenyl porphycenes and porphyrins. *New J Chem*. 2005; 29:378–384.
38. Foley JW, Song XZ, Demidova TN, Jilal F, Hamblin MR. Synthesis and properties of benzo[a]phenoxazinium chalcogen analogues as novel broad-spectrum antimicrobial photosensitizers. *J Med Chem*. 2006; 49:5291–5299. [PubMed: 16913718]
39. Zeina B, Greenman J, Purcell WM, Das B. Killing of cutaneous microbial species by photodynamic therapy. *Br J Dermatol*. 2001; 144:274–278. [PubMed: 11251558]
40. Codling CE, Maillard JY, Russell AD. Aspects of the antimicrobial mechanisms of action of a polyquaternium and an amidoamine. *J Antimicrob Chemother*. 2003; 51:1153–1158. [PubMed: 12697638]
41. Dai T, Tegos GP, Zhiyentayev T, Mylonakis E, Hamblin MR. Photodynamic therapy for methicillin-resistant *Staphylococcus aureus* infection in a mouse skin abrasion model. *Lasers Surg Med*. 2010; 42:38–44. [PubMed: 20077489]
42. Zolfaghari PS, Packer S, Singer M, Nair SP, Bennett J, Street C, Wilson M. *In vivo* killing of *Staphylococcus aureus* using a light-activated antimicrobial agent. *BMC Microbiol*. 2009; 9:27. [PubMed: 19193212]

## Abbreviations

<b>APDT</b>	antimicrobial photodynamic therapy
<b>CFU</b>	colony forming units
<b>DC</b>	dark control
<b>DMA</b>	dimethyl acetamide
<b>DMSO</b>	dimethyl sulfoxide
<b>EDTA</b>	ethylenediamine tetraacetic acid
<b>LC</b>	light control
<b>MRSA</b>	methicillin-resistant <i>Staphylococcus aureus</i>
<b><i>m</i>-THPP</b>	5,10,15,20-tetrakis( <i>m</i> -hydroxyphenyl)-21 <i>H</i> ,23 <i>H</i> -porphine
<b>NTC</b>	non-treated control

<b>PBS</b>	phosphate buffered saline
<b>PDT</b>	photodynamic therapy
<b>PS</b>	photosensitizer
<b>ROS</b>	reactive oxygen species
<b>TMPyP</b>	5,10,15,20-tetrakis( <i>N</i> -methyl-4-pyridyl)-21 <i>H</i> ,23 <i>H</i> -porphine
<b>TPP<sub>o</sub></b>	2,7,12,17-tetraphenylporphycene

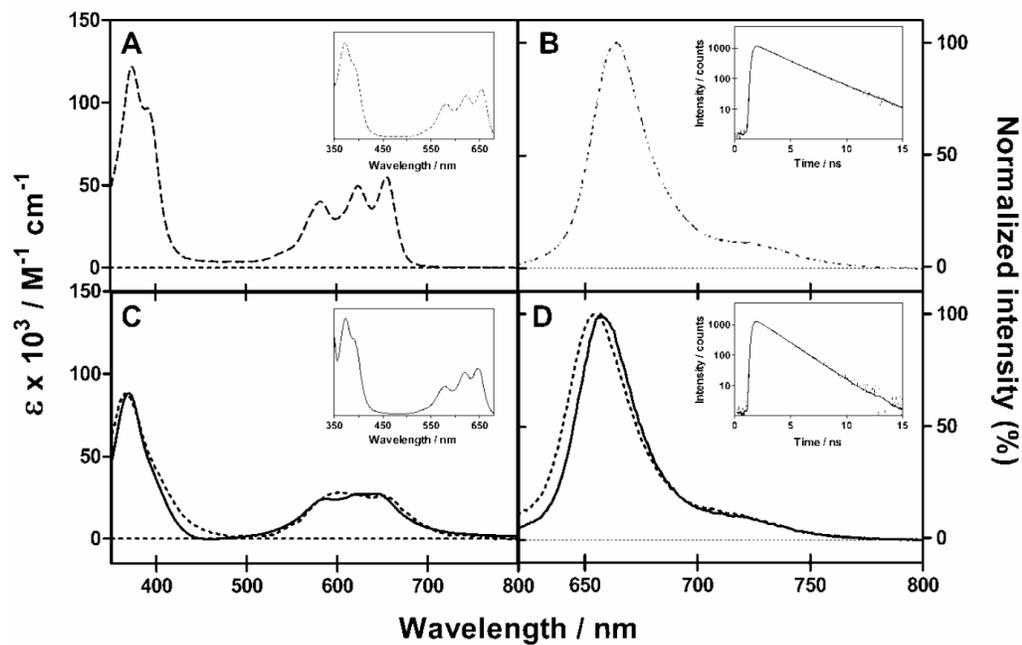


**Figure 1.** (A,C) Absorption and (B,D) fluorescence spectrum of Py<sub>3</sub>MeO-TBPO in (A,B) MeOH and (C,D) water and PBS (solid and dotted line, respectively). Insets: (A,C) Excitation spectrum of the fluorescence at 661 nm. (B,D) Time-resolved fluorescence of Py<sub>3</sub>MeO-TBPO. Signal, fit and instrument response function at 661 nm upon excitation at 375 nm.

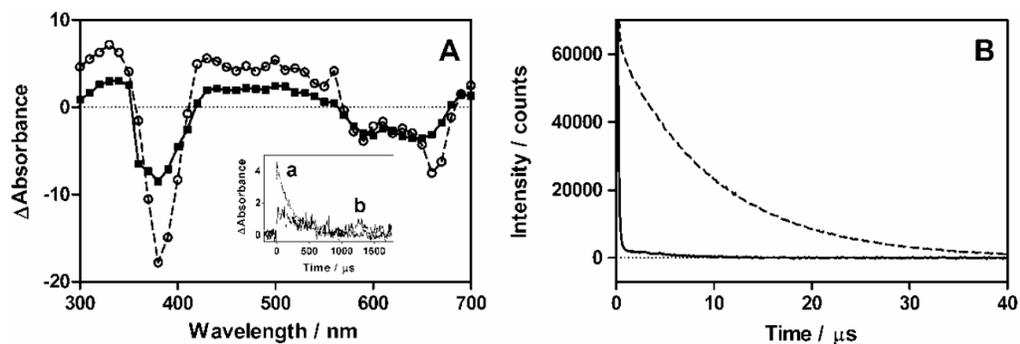


**Figure 2.**

(A) Transient absorption spectrum of the triplet excited state of porphycene 3 in MeOH (grey, dashed line) and water (black, solid line). Inset: Transient absorbance at 420 nm upon excitation at 355 nm in (a) MeOH and (b) water. (B) Singlet oxygen phosphorescence kinetics at 1270 nm of an aqueous solution (solid line) and MeOH solution (dashed line) of  $\text{Py}_3\text{MeO-TBPO}$ .

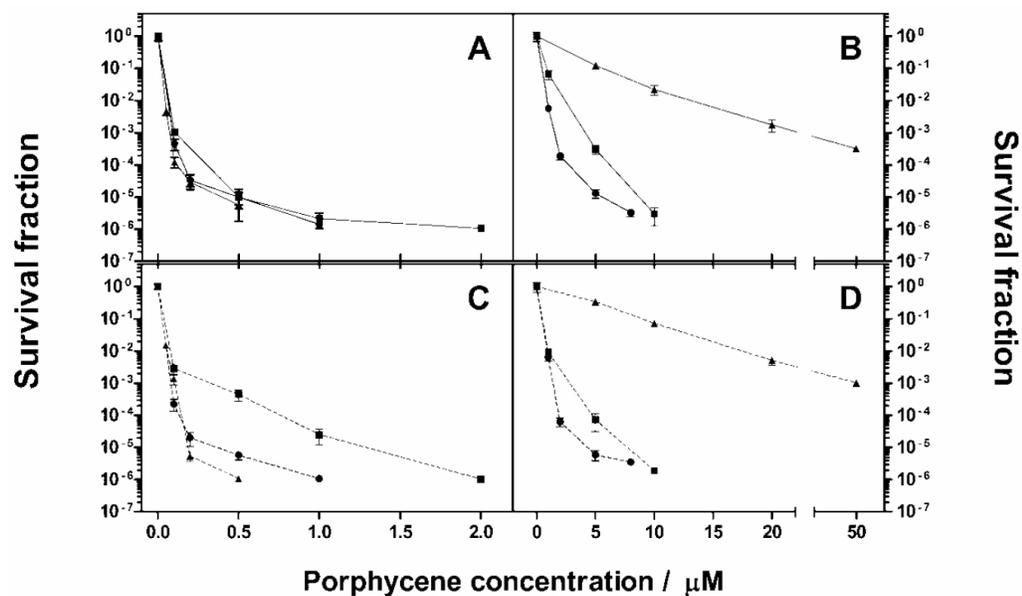


**Figure 3.** Bacterial photoinactivation with  $\text{Py}_3\text{MeO-TBPO}$ . (A,C) Survival curves of MRSA (squares), *S. aureus* (circles), *E. faecalis* (triangles) with (dashed line) and without (solid line) removing the excess of photosensitizer (PS) from the solution after  $30 \text{ J}\cdot\text{cm}^{-2}$  of 652-nm light. (B,D) Survival curves of *A. baumannii* (circles), *E. coli* (squares), *P. mirabilis* (triangles) with (dashed line) and without (solid line) removing the excess of PS from the solution after  $60 \text{ J}\cdot\text{cm}^{-2}$  (*E. coli*) and  $100 \text{ J}\cdot\text{cm}^{-2}$  (*A. baumannii* and *P. mirabilis*) of 652-nm light.

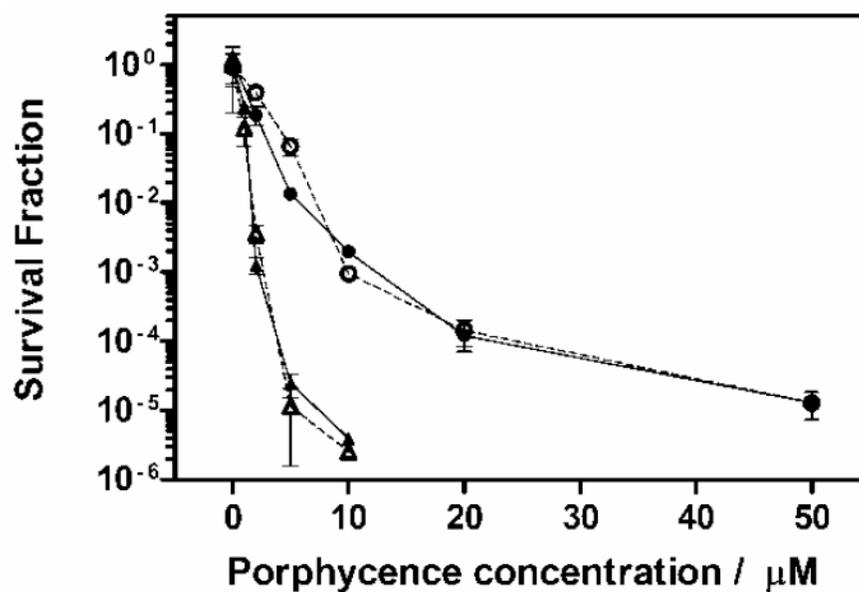


**Figure 4.** Yeast photoinactivation with  $\text{Py}_3\text{MeO-TBPO}$ . Survival curves of *C. albicans* (circles) after  $30 \text{ J}\cdot\text{cm}^{-2}$  of 652-nm light and *C. krusei* (triangles) after  $15 \text{ J}\cdot\text{cm}^{-2}$  of 635-nm light, with (dashed line) and without (solid line) removing the excess of photosensitizer (PS) from the solution.

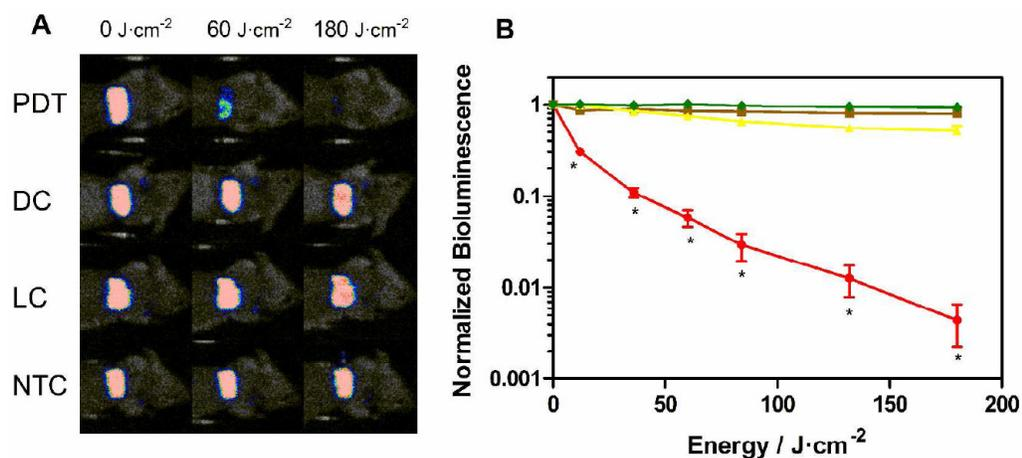


**Figure 5.** *In vivo* MRSA photoinactivation with Py<sub>3</sub>MeO-TBPO. (A) Dose response of bacterial luminescence from burns infected with luminescent MRSA and treated with 100 μM of porphycene 3 and 652 nm light (PDT), with 100 μM of Py<sub>3</sub>MeO-TBPO only (DC), with light (LC) only, and without treatment (NTC). (B) Light-dose response curves of the normalized bioluminescence for mice treated with photodynamic therapy (red), mice treated only with Py<sub>3</sub>MeO-TBPO (brown), mice treated only with light (yellow), and without treatment (green). Every point is an average of five independent mice. \*, *P* < 0.001.

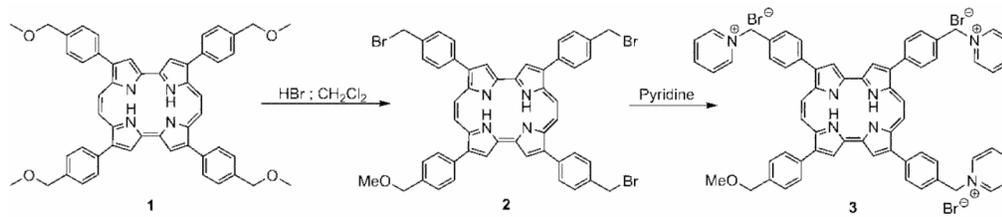
**Scheme 1.**

Table 1

Photophysical properties of Py<sub>3</sub>MeO-TBPO.

Solvent	$\lambda_{\text{abs}} / \text{nm}$	$\lambda_{\text{f}} / \text{nm}$	$\Phi_{\text{f}} [a]$	$\tau_{\text{S}} / \text{ns}$	$\tau_{\text{T}} / \mu\text{s} [b]$	$k_{\text{q}} / \text{M}^{-1}\text{s}^{-1} [c]$	$\Phi_{\text{A}} (\lambda_{\text{exc}} / \text{nm}) [d]$
<b>H<sub>2</sub>O</b>	644	656	0.005	1.8	330	$1.5 \times 10^9$	0.03 (355) 0.004 (532)
<b>MeOH</b>	655	661	0.075	2.6	152	$3.5 \times 10^9$	0.193

[a] Cresil violet was used as reference.

[b] Lifetime of the decays at 420 nm in argon-saturated solutions.

[c] Rate constant for triplet quenching by oxygen. Error bar 10%.

[d] Singlet oxygen quantum yield in air-saturated solutions. Excitation wavelength in parentheses.